The EMBO Journal (2008) 27, 1840–1851 | © 2008 European Molecular Biology Organization | All Rights Reserved 0261-4189/08
www.embojournal.org

THE EMBO JOURNAL

The DNA replication checkpoint aids survival of plants deficient in the novel replisome factor ETG1

Naoki Takahashi[1,2], Tim Lammens[1,2], Véronique Boudolf[1,2], Sara Maes[1,2], Takeshi Yoshizumi[3], Geert De Jaeger[1,2], Erwin Witters[4,5], Dirk Inzé[1,2] and Lieven De Veylder[1,2,*]

[1]Department of Plant Systems Biology, Flanders Institute for Biotechnology, Gent, Belgium, [2]Department of Molecular Genetics, Ghent University, Gent, Belgium, [3]Plant Functional Genomics Research Group, RIKEN Plant Science Center, Yokohama, Japan, [4]Department of Chemistry, Centre for Proteome Analysis and Mass Spectrometry, University of Antwerp, Antwerpen, Belgium and [5]Flemish Institute for Technological Research (VITO), Mol, Belgium

Complete and accurate chromosomal DNA replication is essential for the maintenance of the genetic integrity of all organisms. Errors in replication are buffered by the activation of DNA stress checkpoints; however, in plants, the relative importance of a coordinated induction of DNA repair and cell cycle-arresting genes in the survival of replication mutants is unknown. In a systematic screen for *Arabidopsis thaliana* E2F target genes, the *E2F TARGET GENE 1* (*ETG1*) was identified as a novel evolutionarily conserved replisome factor. ETG1 was associated with the minichromosome maintenance complex and was crucial for efficient DNA replication. Plants lacking the *ETG1* gene had serrated leaves due to cell cycle inhibition triggered by the DNA replication checkpoints, as shown by the transcriptional induction of DNA stress checkpoint genes. The importance of checkpoint activation was highlighted by double mutant analysis: whereas *etg1* mutant plants developed relatively normally, a synthetically lethal interaction was observed between *etg1* and the checkpoint mutants *wee1* and *atr*, demonstrating that activation of a G2 cell cycle checkpoint accounts for survival of *ETG1*-deficient plants.

The EMBO Journal (2008) **27,** 1840–1851. doi:10.1038/emboj.2008.107; Published online 5 June 2008
Subject Categories: cell cycle
Keywords: *Arabidopsis*; DNA replication; DNA replication checkpoint; ETG1; MCM proteins

Introduction

All eukaryotic cells replicate their nuclear DNA in a conserved manner, whereby the parent molecule is unwound and each DNA strand becomes the template for nascent DNA synthesis. For survival, DNA replication must be coordinated with growth and development. In mammals, genetic instability is a hallmark of cancer cells (Bartkova *et al*, 2005; Gorgoulis *et al*, 2005). Therefore, cells have developed signalling cascades to guard against DNA stress. DNA damage and problems of DNA replication activate the ataxia telangiectasia-mutated (ATM) and Rad3-related (ATR) signalling kinases that simultaneously switch on DNA repair genes and arrest cell cycle progression, allowing cells to repair DNA before entering mitosis. ATM responds specifically to double-stranded breaks, whereas ATR primarily senses replication stress caused by blocking of the DNA replication fork progression. Also in plants, ATM and ATR concomitantly induce the expression of DNA repair genes and *WEE1*, which arrests cells in the G2 phase of the cell cycle (Garcia *et al*, 2003; Culligan *et al*, 2004, 2006; De Schutter *et al*, 2007).

Because of its essential role during development, it is not surprising that the molecular machinery controlling DNA replication is highly conserved. Despite the many years of evolution that separate animals from plants, the same E2F/DP pathway regulates entry into S phase by mediating transcriptional induction of genes required for cell cycle progression and DNA replication. The genome of *Arabidopsis thaliana* contains six E2Fs and two DPs (Inzé and De Veylder, 2006). Three E2F proteins (E2Fa, E2Fb, and E2Fc) bind DNA through the consensus E2F-binding site by forming heterodimers with DP proteins (DPa and DPb). Both E2Fa and E2Fb operate as transcriptional activators, whereas E2Fc functions as a repressor (De Veylder *et al*, 2002; del Pozo *et al*, 2002; Rossignol *et al*, 2002; Magyar *et al*, 2005). The remaining *Arabidopsis* E2Fs (E2Fd/DEL2, E2Fe/DEL1, and E2Ff/DEL3) contain duplicated DNA-binding domains, allowing association to consensus E2F sites in an DP-independent manner (Kosugi and Ohashi, 2002; Ramirez-Parra *et al*, 2004; Vlieghe *et al*, 2005).

Both in mammals and *Arabidopsis*, numerous E2F target genes have been identified by using microarrays, chromatin immunoprecipitations (ChIPs), and *in silico* analyses (Ramirez-Parra *et al*, 2003; Dimova and Dyson, 2005; Vandepoele *et al*, 2005). These genes code for proteins that are active during DNA replication, mitosis, DNA checkpoint control, apoptosis, or differentiation. Remarkably, almost every gene encoding a protein involved in licensing for DNA replication is transcriptionally controlled by E2F transcription factors (Vandepoele *et al*, 2005). Licensing for DNA replication is initiated by the formation of the prereplicative complex at replication origins (Gillespie *et al*, 2001; Bell and Dutta, 2002; Diffley and Labib, 2002). First, the origin recognition complex (ORC) proteins bind to DNA during the early G1 to S phase of the cell division cycle. Then, the cell division cycle 6 (CDC6) protein binds to these ORC DNA sites, an event that is followed quickly by binding of chromatin licensing and DNA replication factor 1 (CDT1). Finally, the replication origins are licensed by loading the minichromosome maintenance (MCM) complex to form a prereplicative complex. The MCM complex is a heterohexamer composed of MCM2 to MCM7 and is likely a component of the helicase

*Corresponding author. Department of Plant Systems Biology, VIB, Ghent University, Technologiepark 927, B-9052 Gent, Belgium.
Tel.: +32 9 3313800; Fax +32 9 3313809;
E-mail: lieven.deveylder@psb.ugent.be

Received: 13 February 2008; accepted: 7 May 2008; published online: 5 June 2008

that unwinds DNA during replication (Tye and Sawyer, 2000; Labib and Diffley, 2001; Forsburg, 2004). Once the prereplicative complex is completely formed by the loading of the MCM complexes, the DNA is primed for replication through the action of two conserved protein kinases, the cyclin-dependent kinase (CDK) and Cdc7–Dbf4, with the recruitment of additional replication factors as a consequence to create the preinitiation complex (Kamimura *et al*, 2001; Masumoto *et al*, 2002; Takayama *et al*, 2003; Kanemaki and Labib, 2006). Loading of the preinitiation complex onto the origins activates the MCM helicases and DNA polymerases, resulting in the initiation of DNA synthesis (Zou and Stillman, 2000). After activation of the origins, some of the initiation factors move with the replication forks to support the elongation step of DNA synthesis (Aparicio *et al*, 1997; Takayama *et al*, 2003; Gambus *et al*, 2006; Kanemaki and Labib, 2006).

By studying E2F target genes in *Arabidopsis*, we identified a novel E2F target gene that is directly controlled by the E2Fa and E2Fb transcription factors. Null mutants of this *E2F TARGET GENE 1* (*ETG1*) had a slower cell cycle. Genetic analysis and transcriptional upregulation of the poly(ADP-ribose) polymerase 2 (*PARP2*), *WEE1*, and *RAD51* genes revealed that the cell cycle delay in *etg1* mutant plants was due to the activation of the DNA replication checkpoint. Interestingly, the absence of a functional *ETG1* allele in a *wee1* or *atr* mutant background had a profound impact on plant development, illustrating that the DNA replication checkpoint and, more particularly, its effects on the cell cycle, aids the survival of *ETG1*-deficient plants.

Results

Loss of ETG1 decreases the cell division rate

Previously, we have identified 70 conserved plant E2F target genes (Vandepoele *et al*, 2005). This list holds 40 known regulators of DNA replication and chromatin dynamics, but also 21 genes with unknown function. To identify novel S-

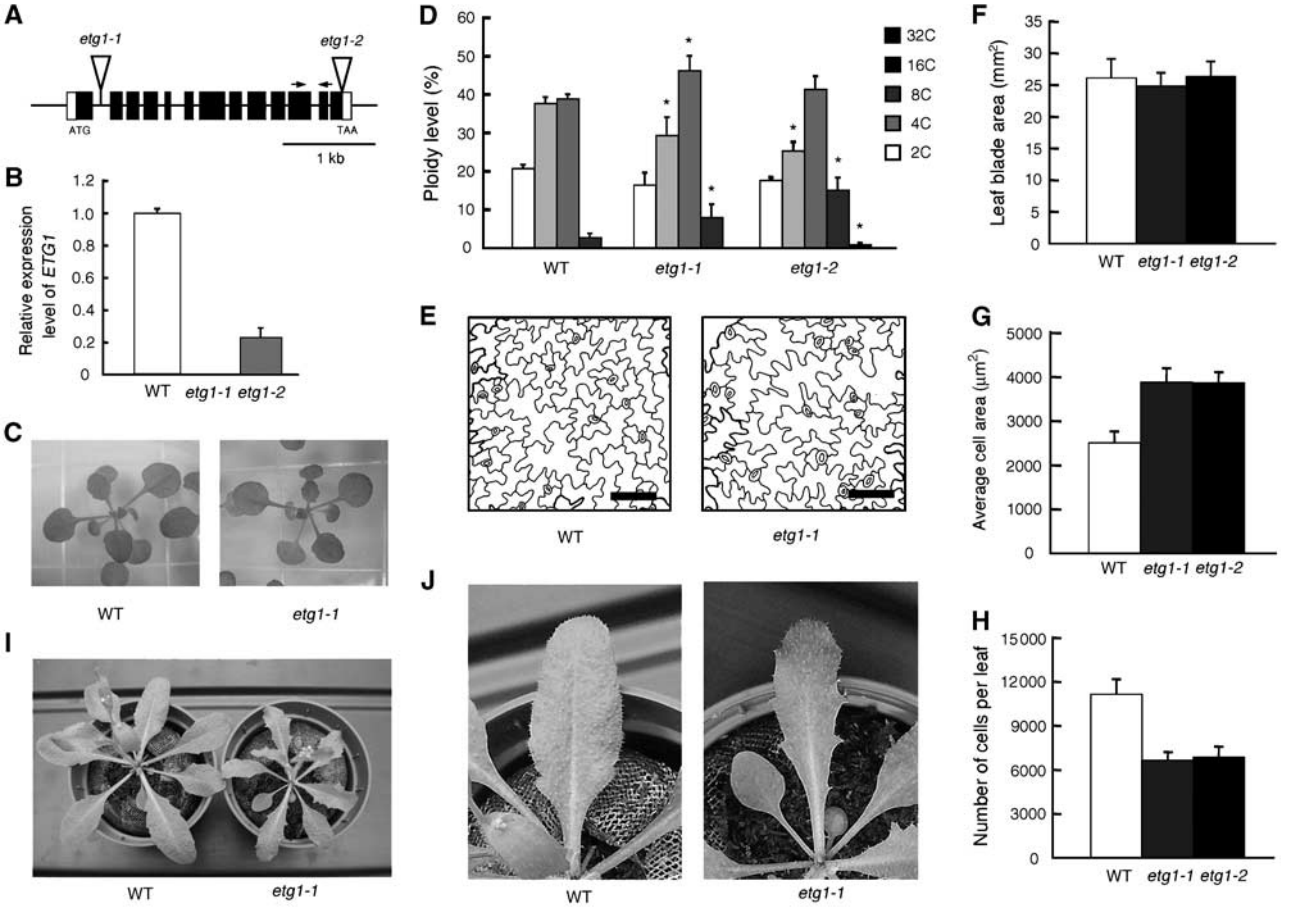

Figure 1 Molecular and phenotypic analysis of *ETG1*-deficient plants. (**A**) Exon (boxes) and intron (lines) structure of *ETG1*. Coding and non-coding regions are shown as black and white boxes, respectively. White triangles and arrows indicate T-DNA insertion sites and primer positions used for real-time RT–PCR analysis, respectively. (**B**) Real-time RT–PCR analysis of *ETG1* expression in wild-type (WT), *etg1-1*, and *etg1-2* plants. Total RNA prepared from first leaves of 9-day-old plants was amplified by RT–PCR. All values were normalized against the expression level of the *ACTIN2* gene. (**C**) Seedling phenotypes of 21-day-old wild-type (WT) and *etg1-1* plants. (**D**) Ploidy level distribution of the first leaves of 3-week-old wild-type (WT), *etg1-1*, and *etg1-2* plants as measured by flow cytometry. Data represent average ± s.d. ($n = 5$). *Significant statistical differences by *t*-test ($P < 0.05$) between wild type and *etg1*. (**E**) Drawing-tube image of the first leaves of 3-week-old wild-type (left) and *etg1-1* (right) plants. Bar = 100 μm. (**F**–**H**) Leaf growth of the first leaf pair of wild-type (WT), *etg1-1*, and *etg1-2* plants. Leaf blade area (F), epidermal cell number (G), and epidermal cell size (H) on the abaxial side of the leaf. Data represent average ± s.d. ($n = 5$). (**I**, **J**) Adult phenotype of wild-type (WT) and *etg1-1* plants. The plants were photographed 5 weeks after germination. (J) Magnification of leaves in wild-type (WT) and *etg1-1* plants.

phase regulatory genes, we screened the latter phenotypically with T-DNA insertion lines. One of the insertion lines showed an endoreduplication phenotype and was designated *E2F TARGET GENE 1* (*ETG1*; At2g40550). To address the role of the *ETG1* gene in plant growth and development, we analysed the loss-of-function effect of *ETG1* with two independent T-DNA insertion lines. The T-DNA was inserted into the first intron (*etg1-1*; SALK_071046) or last exon (*etg1-2*; SALK_145460) of the *ETG1* gene (Figure 1A). *ETG1* transcripts were not detected in the *etg1-1* mutant, whereas the transcript level was 80% reduced in *etg1-2*, when compared to control plants (Figure 1B). In *etg1* mutant seedlings, plant growth appeared macroscopically normal (Figure 1C). However, by comparing the DNA ploidy level of wild-type leaves with that of *etg1-1* and *etg1-2* mutants, the distribution of the C values was slightly, but significantly, changed: in *etg1* mutants, the population of cells with an 8C and 16C DNA ploidy level had increased, demonstrating that deficiency in *ETG1* stimulated endoreduplication (Figure 1D). A similar effect was seen in root tissue (Supplementary Figure S1). The increase in the DNA ploidy level of *etg1* mutants probably originated from an advanced onset of the endocycle, as illustrated by the faster increase in the population of cells with an 8C and 16C DNA content during leaf development (Supplementary Figure S2).

When the first leaf pair from wild-type and *etg1* mutant plants at maturity was compared, the leaf blade area was almost identical for both genotypes (Figure 1F). By contrast, the average abaxial pavement cell area had increased significantly in the mutant plants (Figures 1E and G), accompanied with a decrease in cell number per leaf (Figure 1H). At the bolting stage, younger leaves showed a slightly elongated and serrated leaf phenotype (Figures 1I and J), resembling the phenotype observed in plants whose cell division is inhibited by ectopic expression of the CDK inhibitory gene *KRP2* (De Veylder *et al*, 2001). In addition, the root growth rate of the mutant plants was significantly reduced (Supplementary Figure S3).

To study the effect of loss of *ETG1* function on cell cycle progression in more detail, kinematics of leaf growth was analysed. From day 5 until day 22 after sowing, the first leaves of *etg1-1* and wild-type plants grown side by side under the same conditions were harvested and the leaf blade area and the average cell area of the abaxial epidermal cells was measured by image analysis (De Veylder *et al*, 2001; Boudolf *et al*, 2004). The total cell number was extrapolated as the ratio of leaf blade and average cell areas. Although the leaf blade area was similar in the wild-type and *etg1-1* plants during the whole period of leaf development (Figure 2A), the average cell area, which initially was approximately 100 μm^2 in both plants, increased significantly faster in the *etg1-1* mutant (Figure 2B). The average surface area of *etg1-1* cells was 155% that of wild-type cells at maturity (3880 ± 320 versus $2500 \pm 255\ \mu m^2$). Simultaneously, the number of epidermal cells of *etg1-1* was only approximately 60% that of the wild type (6650 ± 530 versus 11170 ± 1017 cells; Figure 2C). Until day 9 after sowing, the average cell division rate for the whole leaf, calculated on the basis of the increase in cell numbers over time, were constantly lower in the *etg1-1* than in wild-type leaves (Figure 2D). The average cell cycle duration between days 5 and 9, estimated as the inverse of the cell division rate, was significantly longer in the *etg1-1* mutant

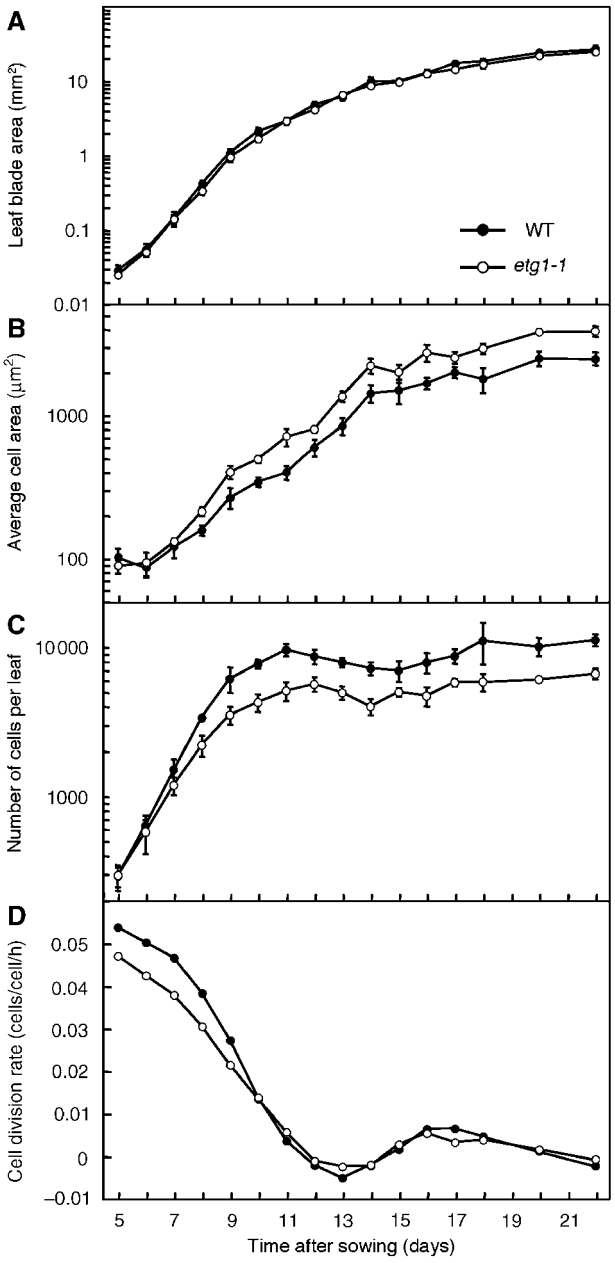

Figure 2 Kinematic analysis of first leaf pair of wild-type (WT) and *etg1-1* plants. (**A**) Leaf blade area. (**B**) Average cell area on the abaxial side of the leaf. (**C**) Number of cells on the abaxial side of leaves. (**D**) Cell division rate. Leaves were harvested at the indicated time points. Data are average ± s.d. ($n = 5$).

(25.3 h) than that in the wild-type plants (21.1 h). In summary, these data illustrate that *ETG1*-deficient plants suffer from a cell cycle delay, with a reduced total cell number that is offset by an enlarged cell size.

Loss of ETG1 function causes a G2 cell cycle arrest

To pinpoint the cell cycle arrest point, we measured the ratio of 4C/2C cells of 8-day-old leaves by flow cytometry. At this time point, leaf cells of both genotypes divide (Figures 2C and D); consequently, 2C and 4C cells represent G1 and G2 cells, respectively. By comparing the ploidy level of wild type and *etg1-1*, a significant increase in the 4C/2C cell ratio was observed (0.29 ± 0.06 and 0.79 ± 0.04 in wild-type and

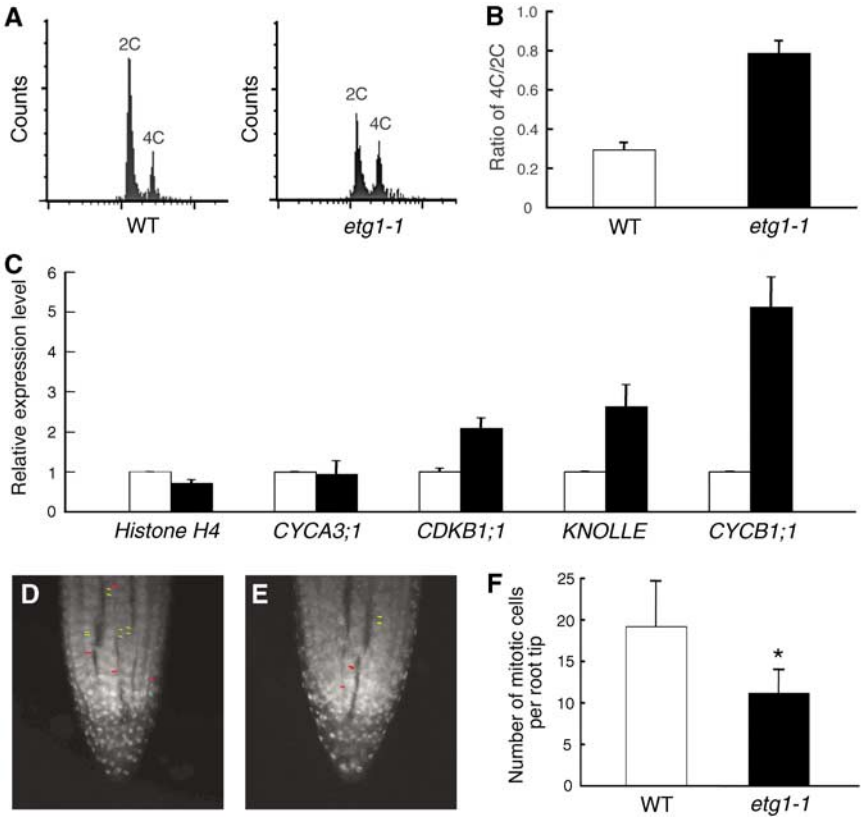

Figure 3 G2 arrest caused by *ETG1* depletion. (**A**) Ploidy-level distribution of the first leaves of 8-day-old wild-type (WT) and *etg1-1* plants as measured by flow cytometry. (**B**) Ratio of 4C/2C cells of the first leaves of 8-day-old wild-type (WT) and *etg1-1* plants. Data represent average ± s.d. ($n = 3$). (**C**) Real-time RT–PCR analysis of S phase (histone *H4* and *CYCA3*;*1*) and G2/M phase (*CDKB1*;*1*, *KNOLLE*, and *CYCB1*;*1*) expression markers in wild-type (white) and *etg1-1* (black) plants. Total RNA prepared from 9-day-old seedlings was amplified by RT–PCR. All values were normalized against the expression level of the *ACTIN2* gene. (**D**, **E**) Distribution of mitotic figures in wild-type (D) and *etg1-1* (E) plants. Metaphase and anaphase/telophase nuclei are false-colored in red and yellow, respectively. (**F**) Number of mitotic cells per root tip of 3-day-old wild-type (WT) and *etg1-1* seedlings. Error bars indicate s.e. ($n = 12$); *Significant statistical differences by *t*-test ($P < 0.05$) between wild type and *etg1-1*.

etg1-1 plants, respectively; Figures 3A and B). These data indicate that the G2-to-M transition was inhibited in the *etg1-1* mutant. Analysis of the expression levels of cell cycle marker genes by real-time reverse transcriptase (RT)–PCR revealed that the transcript level of the G2/M-phase-specific *CYCB1*;*1*, *CDKB1*;*1*, and *KNOLLE* genes had increased in the *etg1-1* mutant, whereas those of the S-phase-specific histone *H4* and *CYCA3*;*1* genes was unaltered (Figure 3C). Despite the increased transcript levels of G2/M-phase-specific genes, a decrease in A-type CDK activity was observed in the *etg1-1* mutant plants (Supplementary Figure S4), in agreement with the observed growth delay and extended cell cycle duration. Counting the number of root cells within the meristem in either metaphase or anaphase/telophase showed that the amount of M-phase nuclei was approximately two-fold lower in the *etg1* mutant than that of wild-type plants (Figures 3D–F). Combined with the observed cell cycle delay, these data indicate a prolonged G2 phase in the *etg1* mutant. More particularly, induction of the *CYCB1*;*1* and *KNOLLE* genes implies that the cell cycle arrest occurs around late G2.

ETG1 transcript is regulated by E2Fa and E2Fb transcription factors

The *ETG1* gene had originally been identified by microarray analysis as an induced transcript in plants ectopically expressing the heterodimeric *E2Fa-DPa* transcription factor (Vandepoele *et al*, 2005). This induction was confirmed by quantitative real-time PCR analysis (Figure 4C). To analyse whether the *ETG1* gene was directly regulated by *E2F* transcription factors, we looked for the presence of consensus E2F-binding sites in its putative promoter region. Two consensus E2F-binding elements were found, ATTCCCGC and TTTCCCGC (158 and 136 bp upstream from the putative start codon, respectively), both in a reverse orientation (Figure 4A). To address whether *ETG1* is an *E2F* target gene *in vivo*, we used ChIP with antibodies against E2Fa, E2Fb, and E2Fc. Promoter fragments of the *ETG1* gene were specifically amplified from the anti-E2Fa and anti-E2Fb immunoprecipitates. These results indicate that *E2Fa* and *E2Fb* can bind directly to the *ETG1* promoter *in vivo*, probably participating in the regulation of its expression. By contrast, the *ETG1* promoter sequences were not recovered from the immunoprecipitates with anti-E2Fc antibodies (Figure 4B). Correspondingly, *ETG1* expression levels were not altered in plants that overexpress *E2Fc* (Supplementary Figure S5).

The regulation of the *ETG1* promoter activity through its E2F consensus sites was further analysed with transgenic plants expressing the β-glucuronidase (GUS) reporter gene under control of the *ETG1* promoter. To define the contribution of each of the E2F-binding sites, we deleted exactly either one (ΔI or ΔII) or both (ΔI, II) of the E2F elements. More than

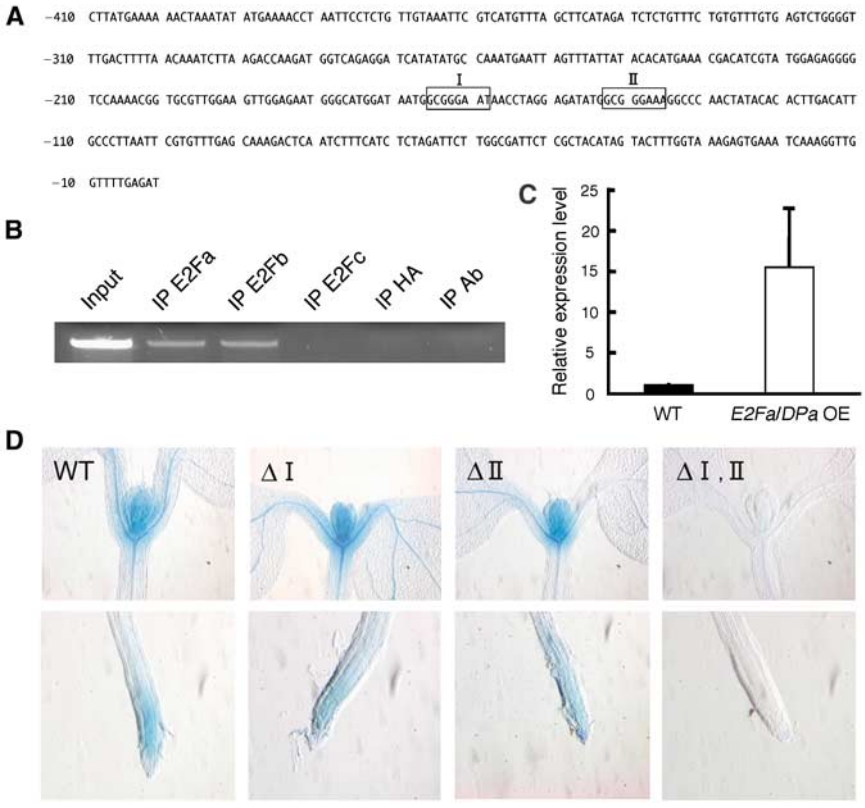

Figure 4 Regulation of *ETG1* gene expression by the *E2Fa* transcription factor. (**A**) Sequence of the *ETG1* promoter showing the presence of two E2F-binding sites at −158 (I) and −136 (II) bp from the ATG translation start codon. (**B**) ChIP assays in 8-day-old *Arabidopsis* plants with antibodies specific for E2Fa, E2Fb, and E2Fc. Precipitation with an anti-HA antibody (IP HA) or without antibody (IP Ab) was used as negative controls. The relative enrichment of genomic fragments of the *ETG1* promoter was estimated by semiquantitative PCR. (**C**) Real-time RT–PCR analysis of *ETG1* expression in wild-type (WT) and *E2Fa/DPa*-overexpressing (*E2Fa/DPa* OE) plants. Total RNA prepared from 6-day-old plants was amplified by RT–PCR. All values were normalized against the expression level of the *ACTIN2* gene. (**D**) Histochemical localization of the GUS activity in transgenic 6-day-old shoot (upper) and root (bottom) apical meristems of seedlings carrying the wild-type (WT) *ETG1* promoter, or a mutant promoter with either one (ΔI or ΔII), or both (ΔI, II) E2F elements exactly deleted.

five independent transgenic lines were analysed per gene construct, all with identical results. In 6-day-old seedlings, high levels of *ETG1* expression were observed in the shoot apical and root meristems (Figure 4D). This expression pattern matched that of the *E2Fa* and *DPa* genes (De Veylder *et al*, 2002). Deletion of either one of the E2F-binding elements (ΔI or ΔII) led to GUS activity patterns identical to those of plants carrying the wild-type *ETG1* promoter (Figure 4D). In contrast, deletion of both E2F-binding elements resulted in a drastic decrease in promoter activity (Figure 4D). These results suggest that E2Fa and E2Fb bind both E2F consensus elements in the *ETG1* promoter and regulate its expression in dividing tissues.

ETG1 is a nuclear protein conserved in eukaryotes

The *ETG1* gene encodes a protein of 598 amino-acid residues (Supplementary Figure S6). ETG1 is a singleton in *Arabidopsis*. No specific amino-acid domain could be identified with the exception of a putative nuclear localization signal, PFKKMKV (amino acids 184–190), suggesting that ETG1 resides in the nucleus. To investigate the subcellular localization of ETG1, a fusion protein of ETG1 and an enhanced green fluorescent protein (eGFP) was transiently produced in leaf epidermal cells of tobacco (*Nicotiana tabacum*). ETG1–eGFP fluorescence was observed in the nucleus only, illustrating that ETG1 is a nuclear protein (Figure 5A). Orthologous proteins of ETG1 were found in rice (*Oryza sativa*; Os01g0166800), human (*Homo sapiens*; C10orf119), mouse (*Mus musculus*; 1110007A13Rik), *Xenopus laevis* (CAJ81286), *Drosophila melanogaster* (CG3430), and fission yeast (*Schizosaccharomyces pombe*; SPAC1687.04) (Supplementary Figure S6), but none in budding yeast (*Saccharomyces cerevisiae*). Interestingly, the transcript of the human *ETG1* is significantly upregulated in brain cancer, breast cancer, and seminoma (http://www.oncomine.org).

ETG1 is a component of the replisome complex and needed for DNA replication

Coexpression patterns can reveal networks of functionally related genes and provide a deeper understanding of processes requiring multiple gene products (Stuart *et al*, 2003; Wei *et al*, 2006). To predict the ETG1 function, we searched for genes coexpressed with *ETG1* by using the ATTED-II coexpression database (Obayashi *et al*, 2007). This search revealed that *ETG1* is highly coexpressed with genes encoding DNA replication proteins, such as the MCM family proteins (MCM2, MCM3, MCM4, MCM5, and MCM7), proliferating cell nuclear antigen proteins (PCNA1 and PCNA2), DNA primase small subunit protein, and DNA polymerase α subunits (Table I). Moreover, when searching for proteins interacting with orthologous ETG1 proteins with the BioGRID protein interactions database (http://www.thebiogrid.org/in-

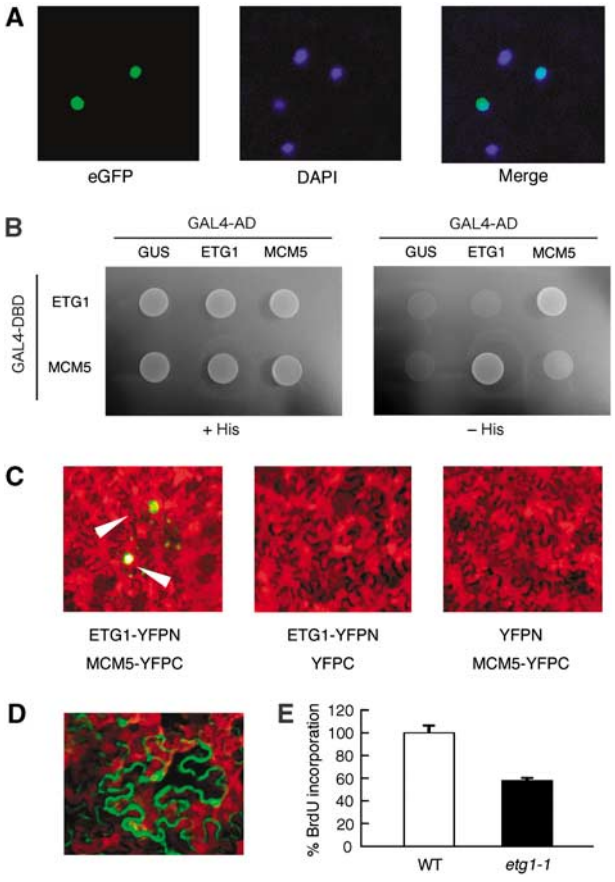

Figure 5 Assembly of ETG1 into the replisome. (**A**) Subcellular localization of ETG1. The full-length ETG1–eGFP fusion protein is localized in the nucleus. (**B**) ETG1 interaction with MCM5 in yeast. Yeast PJ69-4a cells were transformed with a plasmid encoding a fusion between the GAL4 DNA-binding domain and ETG1 and MCM5 (GAL4-DBD–ETG1 and GAL4-DBD–MCM5, respectively). Yeast PJ69-4α cells were transformed with fusions of GAL4 activation domain (AD) with ETG1, MCM5, and GUS as negative controls (GAL4-AD–ETG1, GAL-AD–MCM5, and GAL4-AD–GUS, respectively). Diploid strains were spotted on plates with (+His, positive control) or without (−His) histidine. (**C**) BiFC assay of ETG1 interaction with MCM5 in plant. Tobacco epidermal cells were transfected with a combination of constructs encoding the indicated fusion proteins. YFPN and YFPC are the fragments containing the amino-acid residues 1–154 and 155–238 of YFP, respectively. Arrowheads mark nuclei. (**D**) Subcellular localization of MCM5. The full-length GFP–MCM5 fusion protein was localized in the nucleus and the cytoplasm. (**E**) DNA replication level of the wild-type (WT) and *etg1-1* plants. Seedlings (3 day old) were soaked in BrdU solution for 3 h. Genomic DNA was extracted and the amount of BrdU incorporation was determined by ELISA with an anti-BrdU antibody. The amount of BrdU incorporated into the wild-type plants was arbitrarily set to 100%. Data represent average ± s.d. ($n = 3$).

dex.php), we found that the *Drosophila* orthologue CG3430 interacted with the MCM5 protein. An identical interaction between the *Arabidopsis* ETG1 and MCM5 (At2g07690) proteins was demonstrated with the yeast two-hybrid system (Figure 5B). This protein–protein interaction was confirmed *in planta* by bimolecular fluorescence complementation (BiFC) experiments (Bracha-Drori *et al*, 2004; Walter *et al*, 2004). The sequences coding for ETG1 and MCM5 were fused in frame with either the N-terminal or C-terminal fragment of the yellow fluorescent protein (YFP) (ETG1–YFPN or MCM5-YFPC, respectively). Interaction between the different fusion proteins was tested by introducing them into tobacco leaf epidermal cells. YFP fluorescence was observed in the nuclei of cells transfected with ETG1–YFPN and MCM5–YFPC, demonstrating that the ETG1 protein interacted with MCM5 in the plant nucleus (Figure 5C; ETG1–YFPN and MCM5–YFPC). As expected, no fluorescence was detected when any combination with empty vectors was introduced into tobacco cells (Figure 5C; ETG1–YFPN and YFPC, YFPN and MCM5–YFPC). When the subcellular localization of MCM5 was examined in plants with MCM5–eGFP, the fusion protein MCM5–eGFP resided in both the nucleus and cytoplasm (Figure 5D).

To identify additional ETG1-associated proteins, tandem affinity purification (TAP) was confirmed with MALDI-TOF-TOF-MS-based protein identification (Van Leene *et al*, 2007). *Arabidopsis* cell suspension cultures were stably transformed by *Agrobacterium tumefaciens*-mediated cocultivation with a Pro35S:TAP-ETG1 cassette. On the basis of the presence of the double tag, two-step affinity purification was performed. Besides MCM5, we identified five interacting proteins, including other components of the MCM complex, namely MCM2 (At1g44900), MCM3 (At5g46280), MCM4 (At2g16440), MCM6 (At5g44635), and MCM7 (At4g02060) (Table II; Supplementary Figure S7). Combined with the subcellular localization results, these data indicate that ETG1 assembled into the replisome complex. Therefore, ETG1 depletion was expected to affect the efficiency of DNA replication. This hypothesis was substantiated by the bromodeoxyuridine (BrdU) incorporation rate that was lower in *etg1-1* mutant plants than that in the control plants (Figure 5E). Although this decrease in BrdU incorporation might be unexpected in the light of the observed increase in the endoreduplication level, the reason might be that the endocycle is far slower than the mitotic cell cycle (Beemster *et al*, 2005). Therefore, because of the short labelling period, the BrdU label probably refers to the mitotic S phase only.

ETG1-deficient plants activate the DNA replication checkpoint

Inhibition of DNA replication in *Arabidopsis* results in the simultaneous induction of DNA repair genes and the cell cycle inhibitory *WEE1* gene that arrests cells in the G2 phase of the cell cycle (De Schutter *et al*, 2007). The decreased rate of BrdU incorporation and observed interaction of ETG1 with MCM proteins suggested that the G2 arrest noticed in *ETG1*-deficient plants might be the consequence of replication checkpoint activation. The activation of a cell cycle checkpoint might be the reason for the observed decrease in CDK activity as well. To test this hypothesis, we compared the expression levels of the *RAD51* (DNA repair) and *WEE1* (cell cycle checkpoint) marker genes by real-time RT–PCR in wild-type and *etg1* mutant plants. Ionizing radiation (for example, γ-irradiation and UV light), DNA replication inhibitory drugs (for example, hydroxyurea and aphidicolin), and radiomimetic agents (such as bleomycin) are known to induce *RAD51* and *WEE1* expression (Chen *et al*, 2003; De Schutter *et al*, 2007). Expression of both *RAD51* and *WEE1* was significantly upregulated in the *etg1-1* (Figure 6A) and similarly in *etg1-2* seedlings (data not shown). Activation of the DNA stress

Table I Genes coexpressed with the *ETG1* gene

Rank	Correlation coefficient	Locus	Gene description
1	0.92	At5g46280	Minichromosome maintenance family protein 3 (MCM3)
2	0.90	At1g44900	Minichromosome maintenance family protein 2 (MCM2)
3	0.89	At4g02060	Prolifera protein (PRL)/minichromosome maintenance family protein 7 (MCM7)
4	0.89	At5g41880	DNA primase small subunit
5	0.88	At1g07370	Proliferating cell nuclear antigen 1 (PCNA1)
6	0.88	At2g16440	Minichromosome maintenance family protein 4 (MCM4)
7	0.87	At2g07690	Minichromosome maintenance family protein 5 (MCM5)
8	0.84	At1g67630	DNA polymerase α subunit B
9	0.84	At5g67100	DNA polymerase α catalytic subunit
10	0.83	At2g29570	Proliferating cell nuclear antigen 2 (PCNA2)

Top 10 ranking genes identified by ATTED-II coexpression database.

Table II List of ETG1-copurified proteins identified by MS

Locus[a]	Gene description	SNAPS accession number	Protein MW	Peptide count	Sequence coverage (%)	Protein score/ threshold	Best ion score/ threshold
At1g44900	Minichromosome maintenance family protein 2 (MCM2)	nrAt0.2_52915	105 172	33	43	936/61	104/33
At5g46280	Minichromosome maintenance family protein 3 (MCM3)	nrAt0.2_68302	86 759	14	23	206/61	74/31
At2g16440	Minichromosome maintenance family protein 4 (MCM4)	nrAt0.2_33617	94 168	24	38	696/61	102/28
At2g07690	Minichromosome maintenance family protein 5 (MCM5)	nrAt0.2_19960	81 591	26	38	584/61	107/31
At5g44635	Minichromosome maintenance family protein 6 (MCM6)	nrAt0.2_8374	93 478	20	33	859/61	154/30
At4g02060	Prolifera protein (PRL)/ minichromosome maintenance family protein 7 (MCM7)	nrAt0.2_3907	80 739	26	46	987/61	172/31

[a]All proteins were detected in the two independent TAP experiments.

checkpoint was confirmed by using plants that carried as transgenes promoters of *PARP2* and *WEE1* fused to GUS, which are markers for DNA stress and activation of the replication checkpoint, respectively (Babiychuk *et al*, 1998; Doucet-Chabeaud *et al*, 2001; De Schutter *et al*, 2007). No GUS activity was observed in *PARP2*:*GUS* plants grown under non-stress conditions (Figure 6B). By contrast, treatment of the *PARP2*:*GUS* reporter line with bleomycin resulted in a strong induction of GUS activity (Figure 6D), demonstrating the DNA stress-inducible promoter activity. Similarly, *PARP2* promoter activity was induced in an *etg1-1* background in the absence of any external DNA stress stimulus (Figure 6C). Especially, GUS activity was strongly induced in shoot apical meristem and vascular cells. Analogous results were obtained with *WEE1*:*GUS* reporter plants. In control plants, *WEE1* expression was observed in the shoot apex and vascular cells (Figure 6E; De Schutter *et al*, 2007). This expression pattern was intensified in the *etg1-1* background (Figure 6F), confirming the real-time RT–PCR experiments. The *ETG1* gene itself was not induced under conditions that cause DNA stress, such as γ-irradiation or UV-B treatment (Ulm *et al*, 2004; Culligan *et al*, 2006). Additionally, *etg1-1* mutant plants were not hypersensitive to hydroxyurea or bleomycin (Supplementary Figure S8).

Activation of the DNA replication checkpoint aids the survival of ETG1-deficient plants

DNA replication stress caused by blocking of the replication fork is mainly sensed by the ATR kinase (Culligan *et al*, 2004). Previously, we have demonstrated that the *WEE1* gene is transcriptionally activated upon replication stress in an ATR-dependent manner and transiently arrests cells in the G2 phase, allowing them to finalize DNA replication before proceeding into mitosis (De Schutter *et al*, 2007). When the increased cell cycle duration observed in the *etg1* mutant plants is assumed to result from the activation of the replication checkpoint, *ETG1* deficiency is expected to have a dramatic impact on the development of plants that are unable to arrest their cell cycle in response to DNA stress. To test this hypothesis, double mutants were constructed between *etg1-1* and two DNA stress checkpoint mutants, *atr-2* and *wee1-1*. *WEE1*-deficient plants fail to arrest their cell cycle when DNA replication is perturbed, but DNA repair genes are still induced (De Schutter *et al*, 2007; T Cools, DI and LDV, unpublished data). In contrast, *atr* mutant plants fail both to arrest their cell cycle and to induce repair genes (Culligan *et al*, 2004, 2006). Both *wee1-1* and *atr-2* mutants were hypersensitive to replication-blocking or DNA-damaging drugs, but were viable and developed normally in the absence of exogenous DNA stress treatments (Figures 7A–D). By contrast, *etg1-1 wee1-1* and *etg1-1 atr-2* double mutant plants had a dwarf phenotype under non-stress conditions, illustrating a synthetic interaction between *ETG1* and *WEE1*, or *ATR* (Figures 7E–H). Scanning electron microscopy revealed severe growth suppression (Figures 7I–K). Especially, the size of trichomes was reduced in the double mutants (Figures 7O–Q). No significant difference in leaf epidermal cell shape was observed in *etg1-1 wee1-1* double

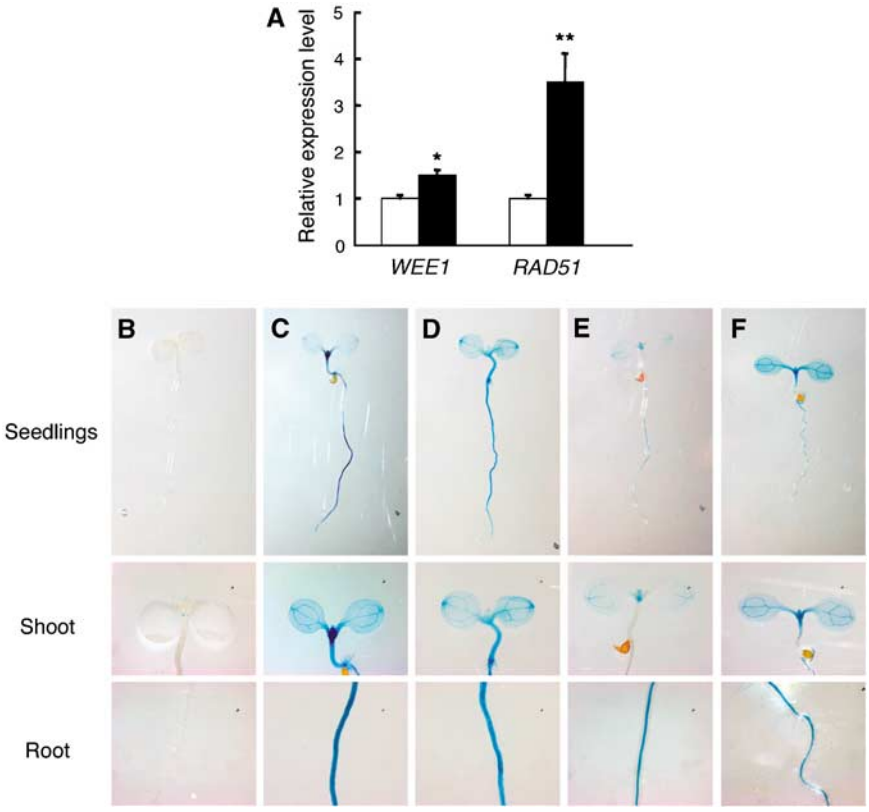

Figure 6 Expression of DNA replication checkpoint and DNA repair genes activated by loss of *ETG1*. (**A**) Real-time RT–PCR analysis of *WEE1* and *RAD51* expression in wild-type (white) and *etg1-1* (black) plants. Total RNA prepared from 9-day-old seedlings was amplified by RT–PCR. All values were normalized against the expression level of the *ACTIN2* gene. * and **Significant statistical differences by *t*-test ($P<0.05$ and $P<0.01$, respectively) between wild-type and *etg1-1*. Data represent average ± s.d. ($n=3$). (**B**–**D**) Histochemical localization of GUS activity in 6-day-old plants harbouring the *PARP2*:*GUS* reporter construct. (B) *PARP2*:*GUS* in a wild-type background. (C) *PARP2*:*GUS* introgressed into *etg1-1*. (D) *PARP2*:*GUS* in a wild-type background in the presence 1 μg ml^{-1} bleomycin. (**E**, **F**) Histochemical localization of GUS activity in 6-day-old plants harbouring the *WEE1*:*GUS* reporter construct in a wild-type background (E) and introgressed into *etg1-1* (F).

mutants, whereas cells lost their jigsaw-like shape in *etg1-1 atr-2* plants (Figures 7L–N). The double mutants arrested at an early stage of development. These results unequivocally indicate that the activation of the DNA replication checkpoint in *etg1* mutant plants is essential for their survival.

Discussion

ETG1 represents a novel component of the replisome

We have identified the ETG1 protein as an important replication factor. We propose that the ETG1 protein is a component of the replication fork that is necessary to maintain genome stability during S phase and that deficiency of *ETG1* might generate DNA damage and genome instability (Figure 8). *ETG1*, originally discovered as a transcript induced in *E2Fa-DPa*-overexpressing plants, was demonstrated to be a direct target gene of the activating *E2Fa/E2Fb* transcription factors. Two E2F-binding sites in the *ETG1* promoter redundantly control *ETG1* expression. Interestingly, not only is the *ETG1* gene highly conserved among species but also E2F-binding sites can be found in the promoter region of *ETG1* orthologues of rice, *Xenopus*, *Drosophila*, mouse, and human. Moreover, in E2F1-depleted cells, transcripts of the *Drosophila ETG1* orthologue (CG3430) are decreased (Dimova *et al*, 2003). Thus, besides the gene product, also the transcriptional control mechanisms that drive *ETG1* expression are conserved, suggesting that E2F-dependent regulation of the *ETG1* expression and of its orthologues is highly important during the replication process.

Our data show that *ETG1* is part of the replisome. First, *etg1* mutants display a clear replication phenotype. Second, both *ETG1* and its *Drosophila* orthologue (CG3430) associate with MCM proteins that bind to the replication origin and travel along the DNA with the remainder of the replication machinery (Kearsey and Labib, 1998; Tye, 1999; Labib *et al*, 2000). Moreover, while this work was in progress, the human orthologous ETG1 has been reported to bind chromatin in a cell cycle phase-dependent manner with the highest affinity for DNA during G1/S and S (Sakwe *et al*, 2007). When the subcellular localization of MCM5 in plants was examined with an MCM5–eGFP fusion protein, MCM5–eGFP was found to reside in both the nucleus and cytoplasm. In yeast, the subcellular localization of the MCM5 protein changes with the cell cycle: it is nuclear between the end of M phase and G1-to-S transition, but is cytoplasmic in other phases of the cell cycle (Hennessy *et al*, 1991). Its dual localization in the nucleus and cytoplasm indicates that a similar situation might hold true for the *Arabidopsis* MCM5 protein. However, by BiFC experiments, we observed that MCM5 and ETG1 interacted only in nuclei and not in the cytoplasm, suggesting an interaction solely when the MCM proteins dock to the replication origins.

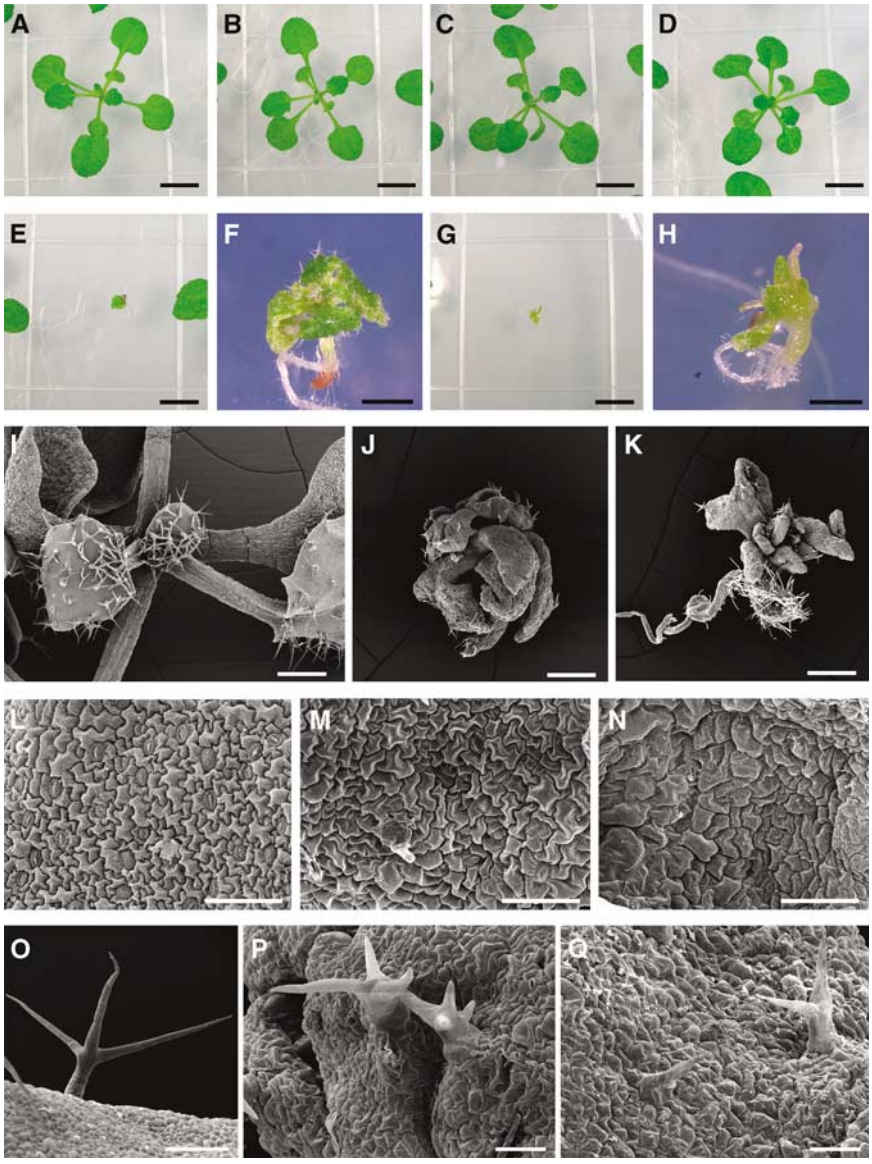

Figure 7 Activation of DNA replication stress checkpoint by ETG1 depletion. Seedling phenotypes of 21-day-old wild-type (Col-0) (**A**), *etg1-1* (**B**), *wee1-1* (**C**), *atr-2* (**D**), *etg1-1 wee1-1* (**E**, **F**) and *etg1-1 atr-2* (**G**, **H**) grown on MS plate. (F, H) Magnification of *etg1-1 wee1-1* and *etg1-1 atr-2* plants, respectively. Scanning electron micrographs of 14-day-old whole seedlings (**I–K**), leaf epidermal cells (**L–N**), and trichomes (**O–Q**). (I, L, O) Wild-type, (J, M, P), *etg1-1 wee1-1*, and (K, N, Q) *etg1-1 atr-2*. Bars = 5 mm (A–E, G), 1 mm (F, H), 500 μm (I–K), 50 μm (L–N, P, Q), and 100 μm (O).

ETG1 deficiency activates a DNA replication checkpoint that accounts for survival

ETG1-deficient plants do not only show a replication defect but also a prolonged G2 phase because of the activation of the DNA replication checkpoint, as illustrated by the upregulation of the DNA repair genes *PARP2* and *RAD51* and the cell cycle checkpoint gene *WEE1*. Despite the prolonged cell cycle duration, resulting in a strongly reduced total cell number, *ETG1* single mutants had a relatively minor developmental phenotype. In contrast, in an *atr* or *wee1* mutant background, *ETG1* deficiency has a huge impact on plant growth with dwarfism, improper cell differentiation, and a developmental arrest as a consequence. These results illustrate that ATR and WEE1 make an essential contribution to the survival of plants without ETG1 function. Previously, lack of ATM or ATR activity has been demonstrated to emphasize the phenotypic defects of telomerase-deficient (*tert*) mutants (Vespa *et al*, 2005). Whereas in a wild-type background, the *tert* mutants display growth and developmental phenotypes from the sixth generation onwards, *tert atm* and *tert atr* double mutants have misshapen leaves, no apical dominance, delayed flowering, and significantly reduced fertility in earlier generations. These data indicate that the activation of the ATM and ATR pathways is required for survival of plants suffering genomic instability. However, it is impossible to attribute the attenuation of the phenotype by functional ATM and ATR to the induction of DNA repair genes, or the ability to arrest cell cycle progression. As *wee1* mutant plants are defective in checkpoint activation but are still able to induce DNA repair genes (De Schutter *et al*, 2007; T Cools, DI, and LDV, unpublished data), the severe phenotype of the *etg1 wee1* double mutants indicates that the activation of the G2 checkpoint

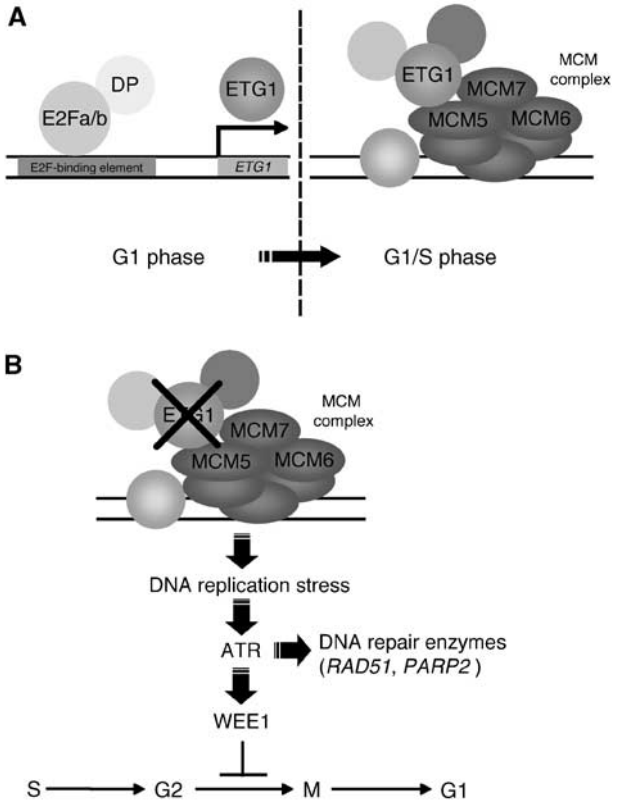

Figure 8 Model for ETG1 function. (**A**) Control of the *ETG1* transcription by E2Fa and E2Fb transcription factors in late G1 phase. ETG1 protein assembles into the DNA replication complex and aids DNA replication during S phase. (**B**) ETG1 depletion causing DNA replication stress and activating the ATR kinase that induces the expression of DNA repair genes, such as *RAD51* and *PARP2*, and the checkpoint kinase *WEE1*. WEE1 arrests cells in the G2 phase of the cell cycle.

contributes mainly to the survival process. Nevertheless, compared to the *etg1 wee1* mutant, the observed growth defects were slightly more outspoken for the *etg1 atr* double mutant, illustrating that the phenotypes resulting from the inability to arrest the cell cycle are partly offset by DNA repair.

Endoreduplication might compensate for reductions in cell number caused by activation of the DNA stress checkpoint

Interestingly, at maturity, the population of cells with a high DNA ploidy level was larger in *etg1* mutant than in control plants, suggesting that the replisome complex of endoreduplicating cells differs from that found in mitotically dividing cells and that ETG1 is not required for the endoreduplication cycle. Previously, DNA double-stranded breaks caused by depletion of the chromatin assembly factor 1 have been found to be accompanied with extra endoreduplication cycles (Endo *et al*, 2006; Exner *et al*, 2006; Ramirez-Parra and Gutierrez, 2007). Additionally, wild-type plants treated with the DNA-damaging drug zeocin significantly increased the DNA ploidy level (Ramirez-Parra and Gutierrez, 2007). The mechanisms that link the maintenance of chromosomal stability with the DNA ploidy level under normal and stressed growth conditions remain unclear. Previously, we have found that the level of A-type CDK activity determines whether a plant cell divides or endoreduplicates (Verkest *et al*, 2005). Therefore, the extra endoreduplication cycles under replication stress might be an indirect effect from the activation of the *WEE1* expression, inactivating the A-type CDK by tyrosine phosphorylation (De Schutter *et al*, 2007). The decrease in CDK activity might prevent entry into mitosis, but still allow S phase to be re-initiated, and, thus, re-replication of the genome. The size of cells has often been found to correlate with their DNA content (Melaragno *et al*, 1993; Folkers *et al*, 1997; Traas *et al*, 1998; Sugimoto-Shirasu and Roberts, 2003). Therefore, in endoreduplicating species the coupling of checkpoint activation with initiation of the endocycle might represent a mechanism by which a reduction in cell number by replication stress is compensated by cell enlargement. Such a coupling might correspond with a survival mechanism allowing plants to achieve a critical biomass required for reproduction, possibly explaining the evolutionary success of the endoreduplication programme among angiosperms.

Materials and methods

Flow cytometric analyses

Leaves were chopped with a razor blade in 300 μl of buffer (45 mM $MgCl_2$, 30 mM sodium citrate, 20 mM 3-[*N*-morpholino]propanesulphonic acid, pH 7, and 1% Triton X-100). To the supernatants, 1 μl of 4,6-diamidino-2phenylindole (DAPI) from a stock of 1 mg/ml was added, which was filtered over a 30-μm mesh. The nuclei were analysed with the CyFlow flow cytometer and the FloMax software (Partec, Münster, Germany). At least three biological and two technical replicates were used for each sample analysed.

Determination of the mitotic index

Roots were fixed in a solution of formaldehyde, ethanol, and acetic acid (2:17:1) for 12 h at 4°C, washed twice in water, and mounted under cover slips. The samples were crushed, snap-frozen with liquid nitrogen to remove the cover slip, and mounted in Vectashield (Vector Laboratories) containing 1 μg/ml DAPI. The roots were analysed for mitotic stages with a Zeiss Axiovert fluorescence microscope.

TAP analysis

TAP experiments were carried out according to Van Leene *et al* (2007). In short, the ETG1-coding sequence was cloned by recombination into the pKNTAP vector, generating a Pro35S:TAP-ETG1 cassette (pKNTAPETG1). *Arabidopsis* cell suspension cultures were stably transformed by *Agrobacterium*-mediated cocultivation with pKNTAPETG1. Transformed *Arabidopsis* cells were selected and transferred to a liquid medium for upscaling. Expression levels of TAP-tagged proteins were checked by protein blotting with an anti-calmodulin-binding protein antibody (data not shown). In the first round of affinity purification, protein extracts of 15 g plant material were incubated with an IgG resin. Bound complexes were released and eluted from the resin by tag cleavage with TEV protease. In the second affinity step on a calmodulin agarose column, co-eluting non-interacting proteins and the TEV protease were removed with the flow-through. Finally, both the ETG1 bait and interacting proteins were eluted from the calmodulin agarose through EGTA-mediated removal of calcium. Eluted proteins were separated on 4–12% NuPAGE gels, excised, and analysed by MALDI-TOF-TOF-MS as described (Van Leene *et al*, 2007). To increase the stringency of the data set, contaminating proteins due to experimental background as determined by Van Leene *et al* (2007) were systematically subtracted from the lists of co-purified proteins.

BrdU ELISA

Seedlings (3 day old) grown on MS agar plates were incubated in the labelling solution with 10 μM BrdU (Roche) at room temperature for 3 h. After treatment, the genomic DNA was extracted with a DNeasy® Plant Mini Kit (Qiagen). The amount of incorporated BrdU was determined by ELISA with an anti-BrdU-POD antibody

(Roche). Three biological and two technical replicates were used at each time point for ELISA. Here, 50 μl of the extracted DNA (0.2 μg/ml) was placed in each well. The ELISA procedure was chiefly that of the 5-bromo-2′-deoxyuridine Labeling and Detection Kit III (Roche).

Supplementary data

Supplementary data are available at *The EMBO Journal* Online (http://www.embojournal.org).

Acknowledgements

We thank Tarik Gaamouche, Amandine Radziejwoski, Shinya Takahashi, Yoshihiro Hase, Eveline Van De Slijke, Jelle Van Leene, Geert Persiau, Ann Pharazyn, and Dominique Eeckhout for technical support, all members of the cell cycle group for fruitful discussions and suggestions, Dr Crisanto Gutierrez for the E2Fc antibody, the Arabidopsis Biological Research Center for providing T-DNA insertion lines, and Martine De Cock for help in preparing the paper. This study was supported by grants from the European Union SY-STEM (MRTN-GT-2004-005336) and the Institute for the Promotion of Innovation through Science and Technology ('Generisch Basisonderzoek aan de Universiteiten' (GBOU) no. 20193 and 20176). TL and TY are indebted to the Institute for the Promotion of Innovation by Science and Technology in Flanders and the Ministry of Education, Science, Sports and Culture for a predoctoral fellowship and a Grant-in-Aid for Young Scientists ((B), 19770044), respectively. LDV is a postdoctoral fellow of the Research Foundation-Flanders.

References

Aparicio OM, Weinstein DM, Bell SP (1997) Components and dynamics of DNA replication complexes in *S. cerevisiae*: redistribution of MCM proteins and Cdc45p during S phase. *Cell* **91:** 59–69

Babiychuk E, Cottrill PB, Storozhenko S, Fuangthong M, Chen Y, O'Farrell MK, Van Montagu M, Inzé D, Kushnir S (1998) Higher plants possess two structurally different poly(ADP-ribose) polymerases. *Plant J* **15:** 635–645

Bartkova J, Hořejší Z, Koed K, Krämer A, Tort F, Zieger K, Guldberg P, Sehested M, Nesland JM, Lukas C, ∅rntoft T, Lukas J, Bartek J (2005) DNA damage response as a candidate anti-cancer barrier in early human tumorigenesis. *Nature* **434:** 864–870

Beemster GTS, De Veylder L, Vercruysse S, West G, Rombaut D, Van Hummelen P, Galichet A, Gruissem W, Inzé D, Vuylsteke M (2005) Genome-wide analysis of gene expression profiles associated with cell cycle transitions in growing organs of Arabidopsis. *Plant Physiol* **138:** 734–743

Bell SP, Dutta A (2002) DNA replication in eukaryotic cells. *Annu Rev Biochem* **71:** 333–374

Boudolf V, Barrôco R, de Almeida Engler J, Verkest A, Beeckman T, Naudts M, Inzé D, De Veylder L (2004) B1-type cyclin-dependent kinases are essential for the formation of stomatal complexes in *Arabidopsis thaliana*. *Plant Cell* **16:** 945–955

Bracha-Drori K, Shichrur K, Katz A, Oliva M, Angelovici R, Yalovsky S, Ohad N (2004) Detection of protein–protein interactions in plants using bimolecular fluorescence complementation. *Plant J* **40:** 419–427

Chen I-P, Haehnel U, Altschmied L, Schubert I, Puchta H (2003) The transcriptional response of *Arabidopsis* to genotoxic stress—a high-density colony array study (HDCA). *Plant J* **35:** 771–786

Culligan K, Tissier A, Britt A (2004) ATR regulates a G2-phase cell-cycle checkpoint in *Arabidopsis thaliana*. *Plant Cell* **16:** 1091–1104

Culligan KM, Robertson CE, Foreman P, Doerner P, Britt AB (2006) ATR and ATM play both distinct and additive roles in response to ionizing radiation. *Plant J* **48:** 947–961

De Schutter K, Joubès J, Cools T, Verkest A, Corellou F, Babiychuk E, Van Der Schueren E, Beeckman T, Kushnir S, Inzé D, De Veylder L (2007) *Arabidopsis* WEE1 kinase controls cell cycle arrest in response to activation of the DNA integrity checkpoint. *Plant Cell* **19:** 211–225

De Veylder L, Beeckman T, Beemster GTS, de Almeida Engler J, Ormenese S, Maes S, Naudts M, Van Der Schueren E, Jacqmard A, Engler G, Inzé D (2002) Control of proliferation, endoreduplication and differentiation by the *Arabidopsis* E2Fa/DPa transcription factor. *EMBO J* **21:** 1360–1368

De Veylder L, Beeckman T, Beemster GTS, Krols L, Terras F, Landrieu I, Van Der Schueren E, Maes S, Naudts M, Inzé D (2001) Functional analysis of cyclin-dependent kinase inhibitors of *Arabidopsis*. *Plant Cell* **13:** 1653–1667

del Pozo JC, Boniotti MB, Gutierrez C (2002) Arabidopsis E2Fc functions in cell division and is degraded by the ubiquitin-SCF^{AtSKP2} pathway in response to light. *Plant Cell* **14:** 3057–3071

Diffley JFX, Labib K (2002) The chromosome replication cycle. *J Cell Sci* **115:** 869–872

Dimova DK, Dyson NJ (2005) The E2F transcriptional network: old acquaintances with new faces. *Oncogene* **24:** 2810–2826

Dimova DK, Stevaux O, Frolov MV, Dyson NJ (2003) Cell cycle-dependent and cell cycle-independent control of transcription by the *Drosophila* E2F/RB pathway. *Genes Dev* **17:** 2308–2320

Doucet-Chabeaud G, Godon C, Brutesco C, de Murcia G, Kazmaier M (2001) Ionising radiation induces the expression of *PARP-1* and *PARP-2* genes in *Arabidopsis*. *Mol Genet Genomics* **265:** 954–963

Endo M, Ishikawa Y, Osakabe K, Nakayama S, Kaya H, Araki T, Shibahara K, Abe K, Ichikawa H, Valentine L, Hohn B, Toki S (2006) Increased frequency of homologous recombination and T-DNA integration in *Arabidopsis* CAF-1 mutants. *EMBO J* **25:** 5579–5590

Exner V, Taranto P, Schönrock N, Gruissem W, Hennig L (2006) Chromatin assembly factor CAF-1 is required for cellular differentiation during plant development. *Development* **133:** 4163–4172

Folkers U, Berger J, Hülskamp M (1997) Cell morphogenesis of trichomes in *Arabidopsis*: differential control of primary and secondary branching by branch initiation regulators and cell growth. *Development* **124:** 3779–3786

Forsburg SL (2004) Eukaryotic MCM proteins: beyond replication initiation. *Microbiol Mol Biol Rev* **68:** 109–131

Gambus A, Jones RC, Sanchez-Diaz A, Kanemaki M, van Deursen F, Edmondson RD, Labib K (2006) GINS maintains association of Cdc45 with MCM in replisome progression complexes at eukaryotic DNA replication forks. *Nat Cell Biol* **8:** 358–366

Garcia V, Bruchet H, Camescasse D, Granier F, Bouchez D, Tissier A (2003) *AtATM* is essential for meiosis and the somatic response to DNA damage in plants. *Plant Cell* **15:** 119–132

Gillespie PJ, Li A, Blow JJ (2001) Reconstitution of licensed replication origins on *Xenopus* sperm nuclei using purified proteins. *BMC Biochem* **2:** 15.1–15.11

Gorgoulis VG, Vassiliou L-VF, Karakaidos P, Zacharatos P, Kotsinas A, Liloglou T, Venere M, DiTullio Jr RA, Kastrinakis NG, Levy B, Kletsas D, Yoneta A, Herlyn M, Kittas C, Halazonetis TD (2005) Activation of the DNA damage checkpoint and genomic instability in human precancerous lesions. *Nature* **434:** 907–913

Hennessy KM, Clark CD, Botstein D (1991) Subcellular localization of yeast *CDC46* varies with the cell cycle. *Genes Dev* **4:** 2252–2263

Inzé D, De Veylder L (2006) Cell cycle regulation in plant development. *Annu Rev Genet* **40:** 77–105

Kamimura Y, Tak Y-S, Sugino A, Araki H (2001) Sld3, which interacts with Cdc45 (Sld4), functions for chromosomal DNA replication in *Saccharomyces cerevisiae*. *EMBO J* **20:** 2097–2107

Kanemaki M, Labib K (2006) Distinct roles for Sld3 and GINS during establishment and progression of eukaryotic DNA replication forks. *EMBO J* **25:** 1753–1763

Kearsey SE, Labib K (1998) MCM proteins: evolution, properties, and role in DNA replication. *Biochim Biophys Acta* **1398:** 113–136

Kosugi S, Ohashi Y (2002) E2Ls, E2F-like repressors of *Arabidopsis* that bind to E2F sites in a monomeric form. *J Biol Chem* **277:** 16553–16558

Labib K, Diffley JFX (2001) Is the MCM2–7 complex the eukaryotic DNA replication fork helicase? *Curr Opin Genet Dev* **11:** 64–70

Labib K, Tercero JA, Diffley JFX (2000) Uninterrupted MCM2–7 function required for DNA replication fork progression. *Science* **288:** 1643–1647

Magyar Z, De Veylder L, Atanassova A, Bakó L, Inzé D, Bögre L (2005) The role of the *Arabidopsis* E2FB transcription factor in regulating auxin-dependent cell division. *Plant Cell* **17:** 2527–2541

Masumoto H, Muramatsu S, Kamimura Y, Araki H (2002) S-Cdk-dependent phosphorylation of Sld2 essential for chromosomal DNA replication in budding yeast. *Nature* **415:** 651–655

Melaragno JE, Mehrotra B, Coleman AW (1993) Relationship between endopolyploidy and cell size in epidermal tissue of Arabidopsis. *Plant Cell* **5:** 1661–1668

Obayashi T, Kinoshita K, Nakai K, Shibaoka M, Hayashi S, Saeki M, Shibata D, Saito K, Ohta H (2007) ATTED-II: a database of co-expressed genes and *cis* elements for identifying co-regulated gene groups in Arabidopsis. *Nucleic Acids Res* **35:** D863–D869

Ramirez-Parra E, Fründt C, Gutierrez C (2003) A genome-wide identification of E2F-regulated genes in *Arabidopsis*. *Plant J* **33:** 801–811

Ramirez-Parra E, Gutierrez C (2007) E2F regulates *FASCIATA1*, a chromatin assembly gene whose loss switches on the endocycle and activates gene expression by changing the epigenetic status. *Plant Physiol* **144:** 105–120

Ramirez-Parra E, López-Matas MA, Fründt C, Gutierrez C (2004) Role of an atypical E2F transcription factor in the control of Arabidopsis cell growth and differentiation. *Plant Cell* **16:** 2350–2363

Rossignol P, Stevens R, Perennes C, Jasinski S, Cella R, Tremousaygue D, Bergounioux C (2002) AtE2F-a and AtDP-a, members of the E2F family of transcription factors, induce Arabidopsis leaf cells to re-enter S phase. *Mol Genet Genomics* **266:** 995–1003

Sakwe AM, Nguyen T, Athanasopoulos V, Shire K, Frappier L (2007) Identification and characterization of a novel component of the human minichromosome maintenance complex. *Mol Cell Biol* **27:** 3044–3055

Stuart JM, Segal E, Koller D, Kim SK (2003) A gene-coexpression network for global discovery of conserved genetic modules. *Science* **302:** 249–255

Sugimoto-Shirasu K, Roberts K (2003) 'Big it up': endoreduplication and cell-size control in plants. *Curr Opin Plant Biol* **6:** 544–553

Takayama Y, Kamimura Y, Okawa M, Muramatsu S, Sugino A, Araki H (2003) GINS, a novel multiprotein complex required for chromosomal DNA replication in budding yeast. *Genes Dev* **17:** 1153–1165

Traas J, Hülskamp M, Gendreau E, Höfte H (1998) Endoreduplication and development: rule without dividing? *Curr Opin Plant Biol* **1:** 498–503

Tye BK (1999) MCM proteins in DNA replication. *Annu Rev Biochem* **68:** 649–686

Tye BK, Sawyer S (2000) The hexameric eukaryotic MCM helicase: building symmetry from nonidentical parts. *J Biol Chem* **275:** 34833–34836

Ulm R, Baumann A, Oravecz A, Máté Z, Ádám É, Oakeley EJ, Schäfer E, Nagy F (2004) Genome-wide analysis of gene expression reveals function of the bZIP transcription factor HY5 in the UV-B response of *Arabidopsis*. *Proc Natl Acad Sci USA* **101:** 1397–1402

Van Leene J, Eeckhout D, Stals H, Persiau G, Van De Slijke E, Van Isterdael G, Laukens K, Remmerie N, Abdelkrim A, Pharazyn A, Van Onckelen H, Inzé D, Witters E, De Jaeger G (2007) Tandem affinity purification of cell cycle protein complexes from *Arabidopsis* cell suspension cultures. *Mol Cell Proteomics* **6:** 1226–1238

Vandepoele K, Vlieghe K, Florquin K, Hennig L, Beemster GTS, Gruissem W, Van de Peer Y, Inzé D, De Veylder L (2005) Genome-wide identification of potential plant E2F target genes. *Plant Physiol* **139:** 316–328

Verkest A, de O Manes C-L, Vercruysse S, Maes S, Van Der Schueren E, Beeckman T, Genschik P, Kuiper M, Inzé D, De Veylder L (2005) The cyclin-dependent kinase inhibitor KRP2 controls the onset of the endoreduplication cycle during Arabidopsis leaf development through inhibition of mitotic CDKA;1 kinase complexes. *Plant Cell* **17:** 1723–1736

Vespa L, Couvillion M, Spangler E, Shippen DE (2005) ATM and ATR make distinct contributions to chromosome end protection and the maintenance of telomeric DNA in *Arabidopsis*. *Genes Dev* **19:** 2111–2115

Vlieghe K, Boudolf V, Beemster GTS, Maes S, Magyar Z, Atanassova A, de Almeida Engler J, De Groodt R, Inzé D, De Veylder L (2005) The DP-E2F-like *DEL1* gene controls the endocycle in *Arabidopsis thaliana*. *Curr Biol* **15:** 59–63

Walter M, Chaban C, Schütze K, Batistic O, Weckermann K, Näke C, Blazevic D, Grefen C, Schumacher K, Oecking C, Harter K, Kudla J (2004) Visualization of protein interactions in living plant cells using bimolecular fluorescence complementation. *Plant J* **40:** 428–438

Wei H, Persson S, Mehta T, Srinivasasainagendra V, Chen L, Page GP, Somerville C, Loraine A (2006) Transcriptional coordination of the metabolic network in Arabidopsis. *Plant Physiol* **142:** 762–774

Zou L, Stillman B (2000) Assembly of a complex containing Cdc45p, replication protein A, and Mcm2p at replication origins controlled by S-phase cyclin-dependent kinases and Cdc7p–Dbf4p kinase. *Mol Cell Biol* **20:** 3086–3096